Multi-mode interference revealed by two photon absorption in silicon rich SiO2 waveguides

S. Manna, F. Ramiro-Manzano, M. Ghulinyan, M. Mancinelli, F. Turri, G. Pucker, and L. Pavesi

Citation: Applied Physics Letters **106**, 071109 (2015); doi: 10.1063/1.4913440
View online: http://dx.doi.org/10.1063/1.4913440
View Table of Contents: http://scitation.aip.org/content/aip/journal/apl/106/7?ver=pdfcov
Published by the AIP Publishing

Multi-mode interference revealed by two photon absorption in silicon rich SiO_2 waveguides

S. Manna,[1,a)] F. Ramiro-Manzano,[1] M. Ghulinyan,[2] M. Mancinelli,[1,a)] F. Turri,[1] G. Pucker,[2] and L. Pavesi[1]
[1]*Nanoscience Laboratory, Dept. Physics, University of Trento, Via Sommarive 14, Povo, I-38050 Trento, Italy*
[2]*Centre for Materials and Microsystems, Fondazione Bruno Kessler, via Sommarive 18, 318123 Povo (Trento), Italy*

(Received 28 January 2015; accepted 11 February 2015; published online 20 February 2015)

Photoluminescence (PL) from Si nanocrystals (NCs) excited by two-photon absorption (TPA) has been observed in Si nanocrystal-based waveguides fabricated by plasma enhanced chemical vapor deposition. The TPA excited photoluminescence emission resembles the one-photon excited photoluminescence arising from inter-band transitions in the quantum confined Si nanocrystals. By measuring the non-linear transmission of waveguides, a large TPA coefficient of β up to 10^{-8} cm/W has been measured at 1550 nm. These values of β depend on the Si NCs size and are two orders of magnitude larger than the bulk silicon value. Here, we propose to use the TPA excited visible PL emission as a tool to map the spatial intensity profile of the 1550 nm propagating optical modes in multimode waveguides. In this way, multimode interference has been revealed experimentally and confirmed through a finite element simulation. © *2015 AIP Publishing LLC*.
[http://dx.doi.org/10.1063/1.4913440]

Non-linear silicon photonics is a rapidly emerging field drawing significant attention due to the possibility of all-optical signal processing employing the existing mature planar Si technology.[1–3] Si photonics involves also the development of new materials to enable functions for which silicon is not ideal. Silicon rich silicon oxide (SRO) matrix containing Si nanocrystals (Si NCs) is one of these materials, which has already shown interesting applications.[4–6] Owing to the significant optical nonlinearities, Si NCs can be chosen as active material in non-linear photonic devices such as switches, routers, and wavelength converters.[7–9] Several papers have reported a third order non-linearity $\chi^{(3)}$ of Si NCs larger than that of bulk silicon, which is explained by both quantum confinement and dielectric mismatch phenomena.[10,11] Specifically, the third order non-linearity can be described by two parameters: the coefficient of non-linear refraction (n_2) and the coefficient of non-linear absorption (β). Therefore, under intense optical excitation, one can write: $n = n_0 + n_2 I$, where n_0 being the linear refractive index and I is the intensity of the laser beam, and $\alpha = \alpha_0 + \beta I$, where α_0 being the linear absorption coefficient. The imaginary part of $\chi^{(3)}$ is related to β by[12]

$$\mathrm{Im}\left[\chi^{(3)}\right] = \frac{4n_0 c}{3\omega_0}\beta, \tag{1}$$

where ω_0 is the laser frequency and c is the light velocity in vacuum.

Specifically, the main contributions to the nonlinear absorption come from two-photon absorption (TPA), excited free carrier absorption and defect-induced absorption. Even though these non-linear absorptions are often considered to be limiting factors, they can be also employed to enable certain functional devices.[13–17] Here, we want to show that TPA allows monitoring the spatial profile of optical modes in waveguides.

With this goal, we studied the non-linear two-photon absorption in single mode and multimode Si NC waveguides. By pulse transmittance measurement through single mode Si NC waveguides, we extract the two photon absorption coefficients and demonstrate TPA-induced photoluminescence (PL) due to inter-band transition in Si NC. Finally, we demonstrate that the TPA induced emission can be used to map the multimode interference (MMI) phenomena in optical waveguides.

The SRO layer was deposited on oxide coated Si wafer using plasma enhanced chemical vapor deposition (PECVD) followed by an annealing at 1150 °C to allow the formation of Si NCs. Sintering at 420 °C in the presence of H_2 was carried out for some wafers with a view to reducing the non-radiative defects via hydrogen passivation. Table I summarizes the different properties of the samples. Waveguides with a typical height of 235 nm and various widths (1–10 μm) were defined by optical lithography and reactive ion etching. Finite element simulation (COMSOL) yields: 1.5 μm wide waveguides are single mode, while 5–10 μm wide waveguides are multimode at 1550 nm. One photon excited PL was studied by surface emission using a 473 nm continuous laser and a Chromex monochromator equipped with a visible-light streak camera. In order to study the TPA in the waveguides, we used a Katana HP 1550 nm laser with a pulse duration of 35 ps at different repetition rates, allowing thus to change both the average as well as the peak powers. Polarizing beam splitter cube along with a $\lambda/2$ plate were used in line of Katana HP to vary the transmitted power through the beam splitter. A hollow core fiber was used to couple the pulsed 1550 nm pump in the waveguide. The transmitted signal was collected through a tapered lens fiber

[a)]Authors to whom correspondence should be addressed. Electronic addresses: smanna@phy.iitkgp.ernet.in and mattia.mancinelli@unitn.it

TABLE I. Sample parameters.

Sample	N_2O(sccm)/SiH_4 (sccm)	PL peak energy (eV)	Refractive index at 1550 nm	Propagation loss, α_0 using cut-back method (dB/cm)	Propagation loss, α_0 calculated from nonlineartransmission (dB/cm)	Two-photon absorption coefficient, β (cm/W)	Im$[\chi^{(3)}]$ (cm^2/W)
G10-sintered	920/92	1.51	1.897	4.0 ± 0.2	5.1 ± 0.1	$(4 \pm 2) \times 10^{-8}$	$(3 \pm 1) \times 10^{-12}$
G10 non-sintered	920/92	1.51	1.897	3.4 ± 0.2	7.7 ± 0.1	$(4 \pm 1) \times 10^{-8}$	$(3 \pm 1) \times 10^{-12}$
G15-sintered	920/65	1.62	1.705	26 ± 1	23 ± 2	$(3 \pm 3) \times 10^{-9}$	$(2 \pm 2) \times 10^{-13}$
G15 non-sintered	920/65	1.66	1.705	22 ± 1	20 ± 2	$(1 \pm 1) \times 10^{-9}$	$(7 \pm 5) \times 10^{-14}$

and analyzed by an optical spectrum analyzer. TPA induced PL emission was collected from the top of the waveguides by a visible Basler Scout camera for imaging purposes. To analyze the luminescence spectra, we have used a ×20 objective to collect the emission, which are reflected by a mirror and sent through a system of lenses to the Chromex monochromator equipped with a visible-light streak camera.

To estimate β, the nonlinear transmission in single mode waveguides with TE polarized light has been studied. Transmission has been analyzed by using[18]

$$\frac{P_{in}}{P_{out}} = \left(\frac{e^{\alpha_0 L} L_{eff}}{A_{eff}} \beta\right) P_{in} + e^{\alpha_0 L}, \tag{2}$$

where P_{in} is the input signal peak power, P_{out} is the transmitted signal peak power, $L_{eff} = (1 - e^{-\alpha_0 L})/\alpha_0$, L is the waveguide length, and A_{eff} is the effective mode area of the waveguide, which is computed by COMSOL simulation. Fitting of P_{in}/P_{out} as a function of P_{in} yields β and α_0.

Figures 1(a) and 1(b) show P_{out} vs. P_{in} as well as P_{in}/P_{out} vs. P_{in} with the linear fits by Eq. (2) for the G10 and G15 sintered waveguides. Results for β are tabulated in Table I. These values are within the range of reported β values, which are in the range of 10^{-7}–10^{-8} cm/W for 813 nm 60 fs laser[7] and of 10^{-6}–10^{-7} cm/W for 1550 nm 4 ns laser for 1250 °C annealed samples.[8,9,19,20] It can be noted that the lower is the Si excess content in the waveguide, i.e., the smaller the Si NC size, the lower is the β value. By using Eq. (1) for the known values of β, the imaginary part of the third order nonlinear susceptibility Im$[\chi^{(3)}]$ has been estimated to be of the order of 10^{-12}–10^{-14} cm^2/W (see Table I).

Figure 2(a) shows the one photon excited photoluminescence spectra of the various samples. According to expectations, the PL spectra of the low Si content G15 sample is blue shifted compared to the high Si content G10 sample. Since the hydrogen passivation does not markedly alter the Si NC, the PL line-shape is not changed from the sintered to the non-sintered sample. The only effect is the increase of the PL intensity (not shown here) owing to the passivation of non-radiative defects. The PL spectra explain the different TPA coefficients observed in the waveguides: The spectral emission region of the G10 waveguide is entirely lower than twice the input signal energy allowing TPA, while this is not verified for the G15 waveguides. This observation is confirmed by TPA excited photoluminescence measurements. When the Si NC waveguides are pumped by a 1550 nm picosecond laser, two photon absorption excites electrons in Si NC. The excited electron relaxes quickly to the minima of the excited state band and decays to the ground state either by photon emission or by a non-radiative process. Figure 2(b) shows the schematic diagram of the setup used to collect TPA assisted PL emission from the top of the Si NC waveguides. A comparison of the one photon excited PL and of the TPA excited PL spectra for G10-sintered waveguides is shown in Fig. 2(c). A small red-shift (∼60 meV) is observed which can be associated to resonant pumping effects.[21]

It is well known that a technique to measure the propagating losses in a waveguide is to monitor the attenuation of the scattered signal light along the waveguide.[12] This method is based on the assumption that the scattered intensity is directly proportional to the intensity of the propagating signal. Here, we make a similar assumption by assuming that the TPA excited PL scattered in a specific point of the

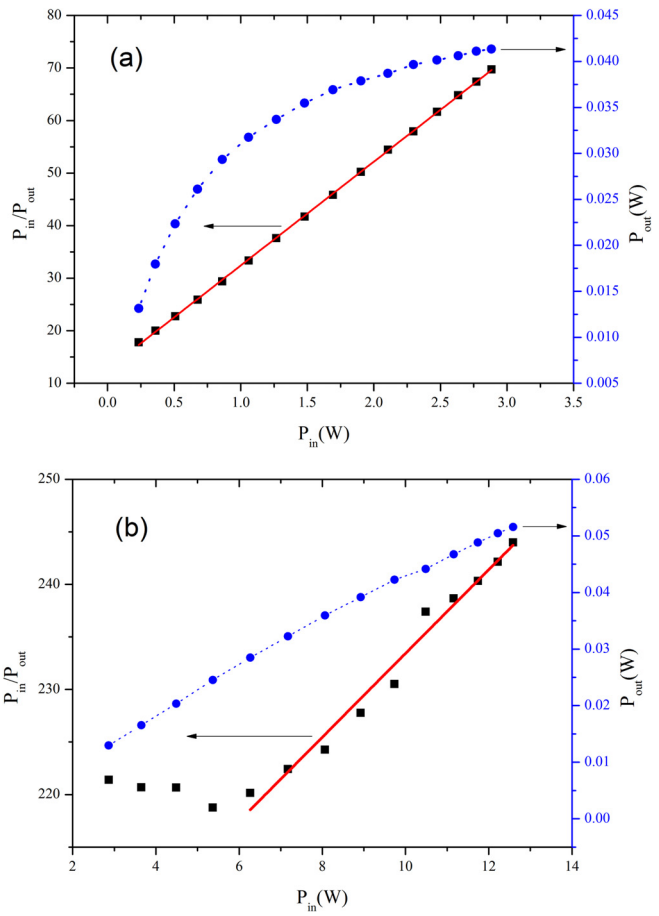

FIG. 1. (a) P_{out} (disks) and P_{in}/P_{out}(black squares) vs. P_{in} for the 1.5 μm wide G10-sintered waveguide. The continuous line is a fit of the data with Eq. (2). (b) The same for the G15-sintered waveguide.

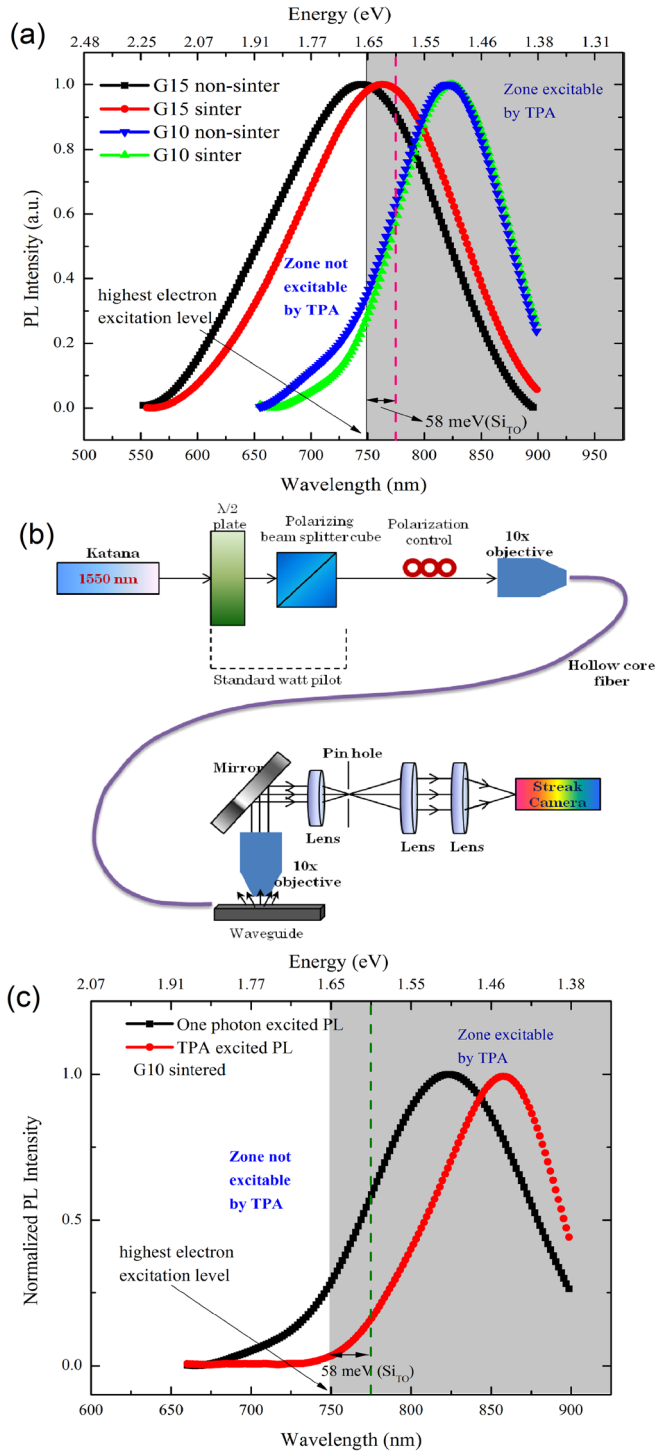

FIG. 2. (a) Normalized one-photon excited photoluminescence spectra of the various Si NC samples excited by a CW 473 nm pump. The grey region shows the region which has an energy lower than two times the energy of 1550 nm photons. (b) Schematic diagram of the setup used for the collection of TPA assisted PL emission from the Si NC waveguides. (c) Comparison between one-photon and two-photon excited PL from the G10-sintered waveguides. The vertical dashed line is twice the energy of 1550 nm photons. Note that the onset of the TPA excited PL is about one TO phonon energy higher than twice the energy of 1550 nm photons.

waveguide surface is proportional to the intensity of the pump signal in that point and it is not due to PL excited elsewhere which has propagated in the waveguide. In fact, at the emission wavelengths, losses as high as 60 dB/cm are characteristics of Si NC waveguides[22] or microdisk resonators.[23]

In this way, by mapping the TPA excited PL at 800 nm, it is possible to map the signal intensity profile at 1550 nm with an improved spatial resolution due to the shorter wavelength of the PL. We do apply this method to map the beating between different modes in a multimode waveguide. Measurements have been performed by imaging the surface of the 5 and 10 μm wide multimode Si NC G10-sintered waveguides through a 20× objective on a visible camera. Results are reported in Fig. 3.

Figure 3(c) shows the visible image of the TPA induced PL emission from the 10 μm G10-sintered waveguide. Clear oscillations in the signal are observed, which are even more evident in the high magnification image in Fig. 3(d). Figure 3(a) shows the integrated TPA excited luminescence intensity versus the position. It is observed that the intensity decreases with the distance due to the signal depletion caused by the nonlinear absorption, weak undulation on the decreasing line are also visible. These become clear oscillations if we integrate the TPA excited PL only in the center of the waveguide (Fig. 3(b)). Oscillations are due to the interference of the propagating optical modes in our multimode waveguide. TPA tracks this multimode interference pattern and so also the TPA excited PL intensity.

Figures 3(e)–3(h) report the same information for the 5 μm wide multimode G10 sintered waveguide. A comparison with the multi-mode interference pattern simulated by using COMSOL for this specific waveguide is shown in Fig. 3(i). In simulation, we neglected losses. The agreement between the measured mode profile and the simulated one is

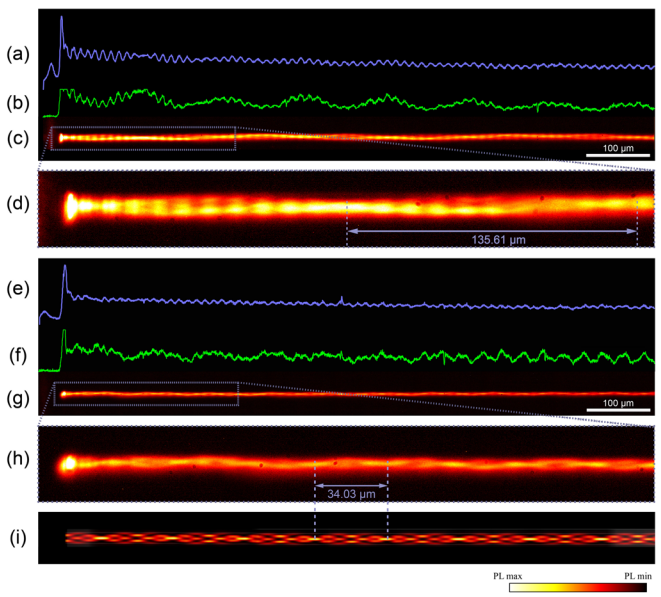

FIG. 3. (a) Integrated intensity profile of the TPA excited PL as a function of the position in the waveguide. Data refer to the 10 μm wide G10-sintered waveguide. (b) Integrated intensity profile of the TPA excited PL as a function of the position when a line scan through the center of the waveguide is performed. (c) TPA excited PL image of the waveguide. (d) Same as (c) but with an increased magnification. The bar refers to the beat length. (e) Integrated intensity profile of the TPA excited PL as a function of the waveguide position. Data refer to the 5 μm wide G10-sintered waveguide. (f) Integrated intensity profile of the TPA excited PL as a function of the position when a line scan through the center of the waveguide is performed. (g) TPA excited PL image of the waveguide. (h) Same as (g) but with an increased magnification. The bar refers to the beat length. (i) COMSOL simulation for the 5 μm waveguide.

remarkable. It is noteworthy that we have not shown the simulation for 10 μm. Compared to the 5 μm waveguide, 10 μm waveguide has larger beat length of MMI (149 μm); so we tried to simulate for this length as well as more also. But even for 149 μm, with our workstation, it is impossible to simulate the system because of the huge amount of memory required.

The experimental beat note data have been extracted by performing a Fast Fourier Transforms (FFTs, shown in Fig. 4) of the integrated spatial profiles of the TPA-PL emission. In the case of the 10 μm waveguide (Figs. 4(a) and 4(b)), one can easily recognize how the beat note emerges (Fig. 4(b), spatial period of 135.61 μm) over the rest of the peaks (Fig. 4(a), FFT of Fig. 3(a)), when only the center of the waveguide is considered (Fig. 3(b)). This behavior is not as evident when the FFT of the 5 μm is analyzed (Figs. 4(c) and 4(d) corresponding to the FFT of the plots of Figs. 3(e) and 3(f), respectively). This is due, on one side, to the lack of high order modes that causes a reduction of the order of the created fold images. As a result, the mirror image (at a special frequency of 34.03 μm) is not as evident. On the other side, defects in the fiber-waveguide coupling cause unbalance of the mode excitation. This yields spatial oscillations in the PL emission image (Figs. 3(a), 3(d) and 3(e), 3(h)). Such a zig-zag pattern impacts more for the small waveguide, inducing spurious peaks in the FFT analysis.

The beat length of the two lowest order modes in a multimode waveguide follows the relation:[24]

$$L_\pi = \frac{\pi}{\beta_0 - \beta_1} \simeq \frac{4 n_r w_e^2}{3\lambda_0}, \tag{3}$$

where β_υ (mode number: $\upsilon = 0, 1$) are the mode propagation constants, n_r is the effective index, w_e is the waveguide width, and λ_0 is the wavelength. For the 10 μm wide waveguide, Eq. (3) yields $L_\pi = 149\ \mu$m, while from the images we extract 135.61 μm. For the 5 μm wide waveguide, Eq. (3) gives $L_\pi = 41\ \mu$m, while experimental $L_\pi = 34.03\ \mu$m. Neglecting the higher order modes in the above equation might explain the difference between experiments and theory. Shortening of the beat length in the narrower waveguide follows self-imaging effect characteristics of MMI.

In conclusion, we have proposed a method to use TPA induced PL to map the spatial multimode interference profile of a Si NC waveguide. The proposed method can be used for other material systems provided that luminescence can be excited by TPA. So, to characterize non-linear TPA, β (TPA coefficient) has been calculated utilizing the transmittance measurement through the Si NC waveguides. Calculated values of β corresponding to 1550 nm wavelength are of the order of 10^{-8}–10^{-9} cm/W, which is more than one order compared to the bulk silicon. We have noticed a change in β as the Si content varies, indicating that the band detuning is responsible for efficient two photon absorptions. For the 5 μm and 10 μm waveguides, the beat lengths of MMI pattern have been found to be 34.03 μm and 135.61 μm, respectively, agreeing well with the theoretical beat lengths. COMSOL simulated MMI pattern of 5 μm waveguide matches well with the experimental one. Scanning near field optical microscopy (SNOM) can be exploited also to map the spatial profile of TPA-PL emission from the top of the waveguide. But characterizing by SNOM could be more difficult compared to our current method since SNOM is limited by very short working area and extremely shallow depth of field, which requires quite long scan time if the sample area is large or meant for high resolution imaging. However, SNOM has a higher spatial resolution compared to our technique.

This work was financially supported by the ITPAR project funded by the Indian DST and the Italian MAE, and by the SIQURO project funded by Provincia Autonoma di Trento. We acknowledge the help of Alessia Guerriero in imaging processing. M.G. and G.P. acknowledge the support

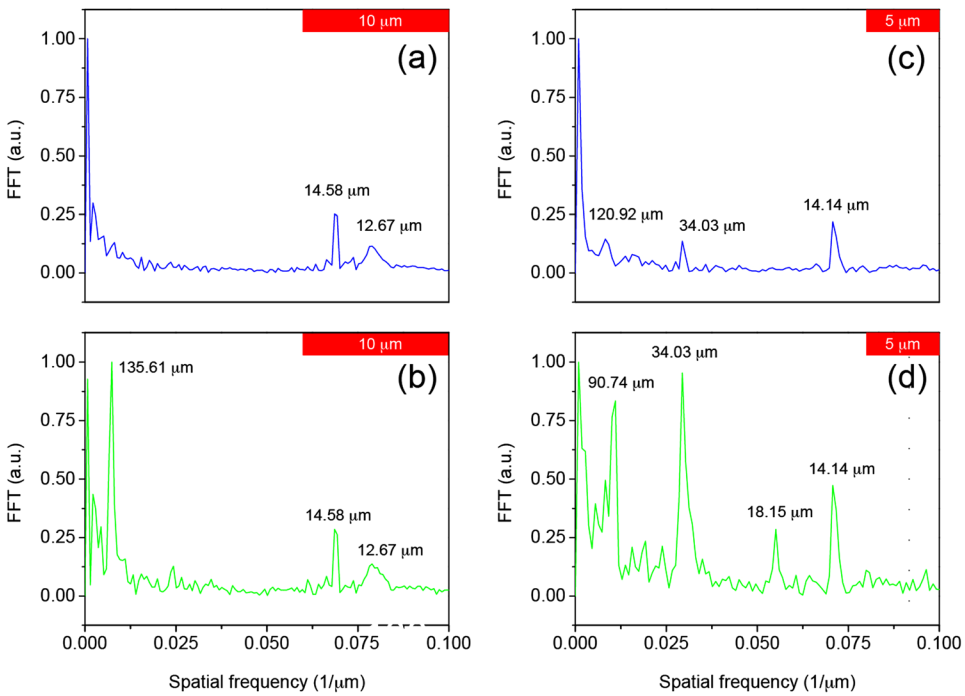

FIG. 4. (a) FFT pattern of the spatial intensity profile of Fig. 3(a) for the 10 μm waveguide, (b) FFT pattern of the spatial intensity profile of Fig. 3(b) for the 10 μm waveguide, (c) FFT pattern of the spatial intensity profile of Fig. 3(e) for the 5 μm waveguide, (d) FFT pattern of the spatial intensity profile of Fig. 3(f) for the 5 μm waveguide.

of the staff of the Microfabrication Laboratory of FBK during sample fabrication.

[1]V. R. Almeida, C. A. Barrios, R. R. Panepucci, and M. Lipson, Nature **431**, 1081 (2004).
[2]M. A. Foster, A. C. Turner, J. E. Sharping, B. S. Schmidt, M. Lipson, and A. L. Gaeta, Nature **441**, 960 (2006).
[3]J. S. Levy, A. Gondarenko, M. A. Foster, A. C. Turner-Foster, A. L. Gaeta, and M. Lipson, Nat. Photonics **4**, 37 (2010).
[4]L. Pavesi, L. Dal Negro, C. Mazzoleni, G. Franzo, and F. Priolo, Nature **408**, 440 (2000).
[5]G. Dehlinger, L. Diehl, U. Gennser, H. Sigg, J. Faist, K. Ensslin, D. Grutzmacher, and E. Muller, Science **290**, 2277 (2000).
[6]H.-S. Han, S.-Y. Seo, and J. H. Shin, Appl. Phys. Lett. **79**, 4568 (2001).
[7]G. Vijaya Prakash, M. Cazzanelli, Z. Gaburro, L. Pavesi, F. Iacona, G. Franzò, and F. Priolo, J. Appl. Phys. **91**, 4607 (2002).
[8]S. Hernández, P. Pellegrino, A. Martínez, Y. Lebour, B. Garrido, R. Spano, M. Cazzanelli, N. Daldosso, L. Pavesi, E. Jordana, and J. M. Fedeli, J. Appl. Phys. **103**, 064309 (2008).
[9]R. Spano, N. Daldosso, M. Cazzanelli, L. Ferraioli, L. Tartara, J. Yu, V. Degiorgio, E. Jordana, J. M. Fedeli, and L. Pavesi, Opt. Express **17**, 3941 (2009).
[10]P. Sanchis, J. Blasco, A. Martinez, and J. Martì, J. Lightwave Technol. **25**, 1298 (2007).
[11]A. Martínez, J. Blasco, P. Sanchis, R. Spano, J. V. Galán, J. García, J. M. Martínez, E. Jordana, P. Gautier, Y. Lebour, R. Guider, P. Pellegrino, S. Hernández, N. Daldosso, B. Garrido, J. M. Fedeli, L. Pavesi, and J. Martí, Nano Lett. **10**, 1506 (2010).
[12]G. P. Agrawal, *Nonlinear Fiber Optics* (Academic Press, New York, 2013).
[13]T. K. Liang, L. R. Nunes, T. Sakamoto, K. Gasagawa, T. Kawanishi, and M. Tsuchiya, Opt. Express **13**, 7298 (2005).
[14]E. Tien, N. S. Yuksek, F. Qian, and O. Boyraz, Opt. Express **15**, 6500 (2007).
[15]T. Tanabe, M. Notomi, S. Mitsugi, A. Shinya, and E. Kuramochi, Opt. Lett. **30**, 2575 (2005).
[16]T. K. Liang, L. R. Nues, M. Tsuchiya, K. S. Abedin, T. Miyazaki, D. Van Thourhout, W. Bogaerts, P. Dumon, R. Baets, and H. K. Tsang, Opt. Commun. **265**, 171 (2006).
[17]R. Salem and T. E. Murphy, IEEE Photonics Technol. Lett. **16**, 2141 (2004).
[18]H. K. Tsang, R. V. Penty, I. H. White, R. S. Grant, W. Sibbett, J. B. D. Soole, H. P. LeBlanc, N. C. Andreadakis, R. Bhat, and M. A. Koza, J. Appl. Phys. **70**, 3992 (1991).
[19]S. Minissale, S. Yerci, and L. Dal Negro, Appl. Phys. Lett. **100**, 021109 (2012).
[20]M. Ito, K. Imakita, M. Fujii, and S. Hayashi, J. Appl. Phys. **108**, 063512 (2010).
[21]L. Pavesi, J. Appl. Phys. **80**, 216 (1996).
[22]P. Pellegrino, B. Garrido, C. Garcia, J. Arbiol, J. R. Morante, M. Melchiorri, N. Daldosso, L. Pavesi, E. Scheid, and G. Sarrabayrouse, J. Appl. Phys. **97**, 074312 (2005).
[23]M. Ghulinyan, D. Navarro-Urrios, A. Pitanti, A. Lui, G. Pucker, and L. Pavesi, Opt. Express **16**, 13218–13224 (2008).
[24]L. B. Soldano and E. C. M. Pennings, J. Lightwave Technol. **13**, 615 (1995).